Journal of Applied Polymer Science

Covalently bound organomodified clay photoinitiators

Barret J. Davidson, Samuel J. Gee, Grayson C. Hurst, Joshua B. Rucker, Jonathan L. Shouse, Joshua B. Smith, T. Brian Cavitt

Department of Chemistry and Biochemistry, Abilene Christian University, Abilene, Texas 79699

Correspondence to: T. B. Cavitt (E-mail: cavitt@chemistry.acu.edu)

ABSTRACT: While organomodified clays are property enhancing additives for composite materials, much of the research thereof has focused on intercalated quaternary ammonium compounds; however, herein the effects of covalently bound organomodified clays (CoBOCs) are explored with particular emphasis on CoBOC photoinitiators. Two commercially available alcoholic photoinitiators (1-hydroxycyclohexyl phenyl ketone and 2-hydroxy-2-methyl-1-phenylpropanone) were reacted with isophorone diisocyanate to form half-adducts and then reacted with Cloisite 93A, an organophilic montmorillonite clay, to form two CoBOC photoinitiators. The CoBOC photoinitiators were integrated into a standard formulation and subsequently ultraviolet (UV) cured. Property characterization thereof (e.g., adhesion, hardness, and flexibility) yielded unchanged or increased properties with the exception of impact flexibility. Finally, the CoBOC photoinitiators were kinetically characterized via photo-differential scanning calorimetry (photo-DSC) within 1,6-hexanediol diacrylate (HDODA). While increasing concentrations of clay additives generally decrease polymerization rates, increasing concentrations of the CoBOC photoinitiators exhibited increased polymerization rates. Therefore, the CoBOC photoinitiators can enhance the polymerization kinetics and physical properties of UV-curable coatings. © 2015 Wiley Periodicals, Inc. J. Appl. Polym. Sci. **2015**, *132*, 41883.

KEYWORDS: clay; coatings; composites; photopolymerization; properties and characterization

Received 29 July 2014; accepted 13 December 2014

DOI: 10.1002/app.41883

INTRODUCTION

Barrier coatings, also called encapsulants, are an enabling technology for many industrial and consumer applications including food and medical packaging, photovoltaics (i.e., solar cells), flexible electronics, electronic displays, batteries, and many more. Though barrier coatings are an enabling technology for many electronics applications, they are also a limiting technology as exemplified by the exceptionally low water vapor transmission rate (WVTR), less than 10^{-6} g/m^2/day, and oxygen transmission rate (OTR), 10^{-3} cm^3/m^2/day, recommended for some applications involving organic light emitting diodes (OLEDs) and photovoltaic cells.[1]

No low-cost, easily mass produced organic or organic-inorganic hybrid barrier material currently meets the aforementioned ultra-low WVTR; however, the WVTR varies widely from application to application.[1] In other words, if a developed barrier coating does not quite meet the recommended threshold for one application (e.g., OLEDs with WVTR less than 10^{-6} g/m^2/day), the coating will likely meet the threshold for another application (e.g., electrophoretic displays with WVTR less than 10^{-2} g/m^2/day). Furthermore, the electronic barrier coating market is predicted to grow exponentially with a predicted $3.4 billion in global sales in 2019, a tenfold increase from predicted 2014 sales.[1]

While a low-cost, high throughput, effective organic or organic–inorganic hybrid barrier coating has not been developed, the answer may be found with appropriate clay composite materials. Clay composite materials continue to be of interest to the discipline due to the economic and physical advantages of related products. Many of these clay composite materials may undergo an intercalation (i.e., spreading via insertion of compatible compounds between the clay platelets) or exfoliation process (i.e., separation of the clay platelets) whereupon they may be characterized as nanocomposite materials with exceptional properties, depending on the interplate d-spacing (Figure 1).[2–22]

If exfoliated clay was used as a portion of the barrier coating, the resulting nanoplates could act as a physical barrier to water and oxygen permeation by providing a tortuous path.

Recently, the literature has been filled with clay composite materials used in photopolymerization.[2–21,23–28] The vast majority of the literature discusses the physical functionalization of the clays via ion exchange methods to introduce either polymerizable monomers, film-forming additives, or, in rare cases,

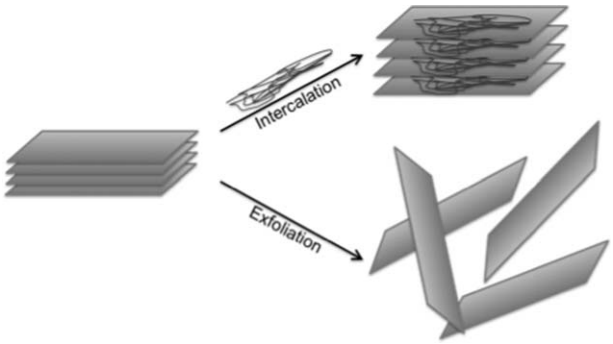

Figure 1. Clay platelet exfoliation and intercalation.

photoinitiators whereupon the ion exchange functionalization produces an organic-inorganic hybrid material that is more readily integrated or compatiblized into the formulation and resulting polymer.[4–9,16–21,23–26,29] For example, Tan *et al.*[9] reported the functionalization of an alcoholic photoinitiator (i.e., 2-hydroxy-2-methyl-1-phenylpropanone) via the isocyanate-alcohol reaction to form a tetrasubstituted silane followed by sol–gel reaction with an ammonium silane and subsequent intercalation into montmorillonite. However, ion exchange methodologies have added cost and often yield compounds that are extractable from the final polymer material. Such extractables could pose health risks and weakened physical properties.

Direct, covalent functionalization of clays are much rarer than the ion exchange modification of the clays. Jlassi *et al.*[3] functionalized pyrrole with a silane which covalently bound the pyrrole to the clay and thereafter was polymerized to form polypyrrole. Lv *et al.*[2] illustrated that the inorganic crystal structure of a montmorillonite clay containing hydroxide groups in the crystal lattice may be functionalized using common urethane formation reactions to form covalently bonded organic-inorganic hybrid materials capable of exfoliation on polymerization.

The project's purpose is to design and characterize a series novel organomodified clay photoinitiators incorporated into barrier coatings or encapsulants as a composite material. To accomplish the aforementioned purpose several systematic objectives were completed. First, two half-adducts were successfully synthesized and characterized from the reaction of isophorone diisocyanate with two commercially available alcohol-functionalized photoinitiators. Second, the two half-adducts were further reacted with an organophilic montmorillonite clay and subsequently characterized, producing a functionalized covalently bound organomodified clay (CoBOC) photoinitiator from each of the half-adducts. Third, each of the CoBOC photoinitiators were incorporated at varying concentrations into a standardized formulation, ultraviolet (UV) irradiated to cure the formulations, and thereafter physically characterized based on ASTM standards. Generally, the physical properties were either comparable or improved relative to the controls. Finally, kinetic characterization was performed by varying concentrations of the CoBOC photoinitiators and performing a comparative analysis of the overall photopolymerization rate. Results demonstrated increasing polymerization rates for increasing CoBOC photoinitiator concentrations.

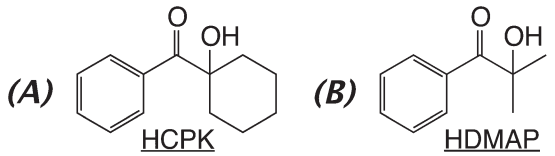

Figure 2. Photoinitiator structures: (A) HCPK and (B) HDMAP.

EXPERIMENTAL

Materials

Photoinitiators [1-hydroxycyclohexyl phenyl ketone (HCPK) and 2-hydroxy-2-methyl-1-phenylpropanone (HDMAP)] were donated by IGM Resins as were trimethylolpropane triacrylate [Photomer 4006 (TMPTA)] and an aliphatic urethane diacrylate oligomer [Photomer 6210 (AUDA); Figure 2].

Isophorone diisocyanate (IPDI), used as a reactive linker, was provided by Bayer Material Science. Southern Clay Products supplied Cloisite 93A (C93A), an organophilic, ternary ammonium methyl tallow salt modified montmorillonite clay. All other materials were purchased from Aldrich. C93A was stored in a dessicator containing anhydrous calcium chloride to minimize water uptake. All other materials were used as received from the supplier.

Synthesis of Half-Adducts

The synthesis of the half-adducts (Scheme 1) largely followed a procedure reported in the literature.[30] An addition funnel and a condenser, fitted with an anhydrous calcium chloride drying

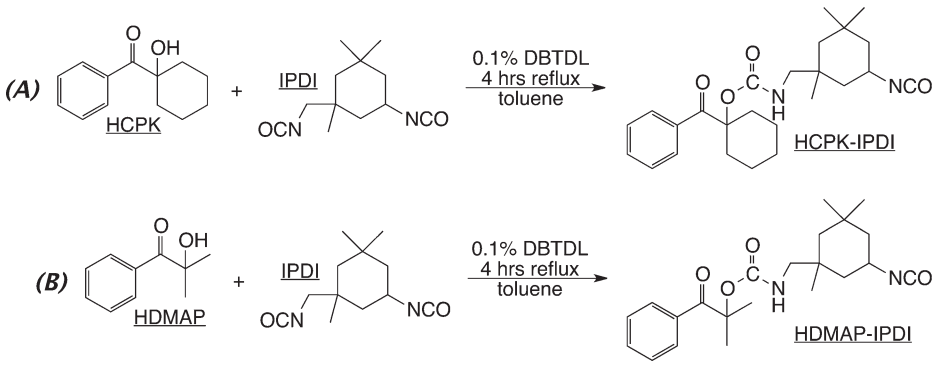

Scheme 1. Synthesis of half-adducts: (A) HCPK-IPDI and (B) HDMAP-IPDI.

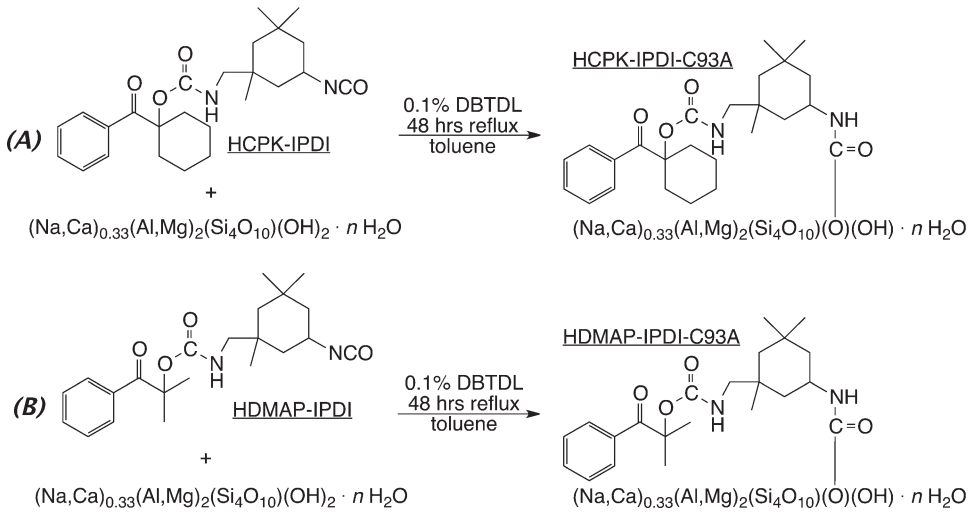

Scheme 2. Synthesis of CoBOC photoinitiators: (A) HCPK-IPDI-C93A and (B) HDMAP-IPDI-C93A.

tube, were attached to a Claisen head connected to a 250 mL round-bottom flask equipped with a magnetic stir bar. IPDI (100 mmol) and toluene (40.0 mL) was added to the flask. Into the addition funnel, the photoinitiator (100 mmol) was dissolved in 40.0 mL toluene to which was added 0.1 wt % of a catalyst [dibutyl tin dilaureate (DBTDL)]. The contents of the addition funnel were added dropwise to the flask containing IPDI and toluene while stirring at room temperature. After dropwise addition, the resulting solution was refluxed with stirring in an oil bath (130°C) for 4 h to complete the synthesis of the half-adducts: HCPK-IPDI and HDMAP-IPDI. Structure was confirmed via IR and ^{1}H-NMR spectroscopies. The disappearance of the alcoholic proton (i.e., OH singlet) for HCPK and HDMAP at 3.3 and 4.8 ppm, respectively, and the appearance of the NH of the two constitutional urethane isomers provide evidence for the described reaction.

Due to the elevated temperature and the high reactivity of the isocyanate groups, the synthesized half adducts are a mixture of two constitutional urethane isomers formed by the reaction of the alcohol with either the primary or secondary isocyanate as indicated by the presence of two similar NH singlets and two similar CH_2 singlets in the ^{1}H-NMR. For the HCPK-IPDI constitutional isomers, the chemical shifts of the NH singlets are 5.1 and 4.9 ppm; the CH_2 singlets appear at chemical shifts of 2.98 and 2.87 ppm. Likewise, the chemical shifts for the HDMAP-IPDI constitutional isomers are 5.2 and 5.1 ppm for the NH singlets and, for the CH_2 singlets, 2.95 and 2.85 ppm.

HCPK-IPDI half-adduct ($C_{25}H_{34}N_2O_4$) ^{1}H-NMR (60 MHz, $CDCl_3$, δ) 8.05 (m, 2H, Ar H), 7.4 (m, 3H, Ar H), 5.1 and 4.9 (s, 1H, NH), 3.3 (m, 1H, CH), 2.98 and 2.87 (s, 2H, CH_2), 1.65 (m, 6H, CH_2), 1.2 (m, 10H, CH_2), 0.9 (t, 9H, CH_3).

HDMAP-IPDI half-adduct ($C_{22}H_{30}N_2O_4$) ^{1}H-NMR (60 MHz, $CDCl_3$, δ) 8.0 (m, 2H, Ar H), 7.4 (m, 3H, Ar H), 5.2 and 5.1 (s, 1H, NH), 3.5 (m, 1H, CH), 2.95 and 2.85 (s, 2H, CH_2), 1.7 (m, 6H, CH_2), 1.3 (s, 6H, CH_3), 0.9 (t, 9H, CH_3).

Table I. Percent Composition in Formulations

	Formulation					
Compound	α	β	γ	δ	ε	ζ
AUDA	66.0	66.0	64.7	64.7	65.3	65.3
TMPTA	33.0	33.0	32.3	32.3	32.7	32.7
HCPK	1.0		1.0			
HDMAP		1.0		1.0		
C93A			2.0	2.0		
HCPK-IPDI-C93A					2.0	
HDMAP-IPDI-C93A						2.0
Totals	100.0	100.0	100.0	100.0	100.0	100.0

Synthesis of CoBOC Photoinitiators

The synthesis of the CoBOC photoinitiators (Scheme 2) generally followed a previously reported procedure.[2] The flask containing the aforementioned half-adduct solution remained in the oil bath (130°C) while the clay (4.00 g C93A) was then added via a powder funnel with stirring to the solution and refluxed with stirring for 48 h. The CoBOC photoinitiators (i.e., HCPK-IPDI-C93A and HDMAP-IPDI-C93A) were isolated via suction filtration and then rinsed several times with chloroform to remove residual unreacted half-adduct and DBTDL. The CoBOC photoinitiators were then air dried on a watchglass. Due to the insolubility of the CoBOC photoinitiators, structure confirmation was only performed via solid state IR spectroscopy (KBr pellet).

X-ray Fluorescence

Samples were prepared by placing 6.5 g of the sample (C93A and HCPK-IPDI-C93A) into an aluminum sample cup and inserted into a Spex SamplePrep X Press (Model 3635). Each sample had 30 tons of pressure applied for 30 s; the applied pressure was then released over 30 s. The pressed samples were inserted into a Rigaku NEX CG to obtain semi-quantitative (for elements more massive than neon) elemental composition via energy dispersive X-ray fluorescence (ED-XRF) using an X-ray

Table II. Relevant IR Peak Locations for Differentiating Synthetic Products

Peak	Wavenumber range (cm^{-1})	Bands
1	3628	O—H stretching of structural hydroxyl group
2	3455-3421	H—OR hydrogen bonded stretch
3	3371-3369	H—NR_2 hydrogen bonded stretch of urethane group
4	2267-2256	Isocyanate
5	1717-1720	C=O stretching (urethane)
6	1670-1677	C=O stretching (photoinitiator)
7	1110	Si—O in plane stretching
8	1093	Si—O out of plane stretching
9	780, 700	Monosubstituted aromatic out of plane bend

tube with a palladium anode (50 kV, 1 mA) and under a helium atmosphere.

Formulations

Standard formulations used a 2 : 1 oligomer/monomer mixture of an aliphatic urethane diacrylate oligomer (AUDA) and trimethylolpropane triacrylate (TMPTA). One set of control formulations used 1% by weight photoinitiator (HCPK or HDMAP) and the aforementioned oligomer/monomer mixture. The other set of control formulations was identical to the first control set with the addition of 2% C93A by weight. The test samples were comprised of the CoBOC photoinitiators (2% by weight) and the oligomer/monomer mixture. Formulations comprised, in part, of either the clay and CoBOC photoinitiators were sonicated to break up the macroaggregates. All formulations were applied to Q Panel stainless steel plates at a 4 mil (100 μm) thickness. Table I details the formulation compositions.

UV Curing

The formulations were cured in multiple passes in an air atmosphere using a Fusion UV Systems, Inc. LC-6/F300S (H-bulb) at 21 ft/min until passing the traditional thumb-twist test.

Physical Characterization

Multiple ASTM techniques were used to physically characterize the final coatings including crosshatch adhesion, pencil hardness, impact flexibility (direct and reverse), and flexibility via the conical mandrel (compression and elongation).[31–34]

Kinetic Characterization

Photo-differential scanning calorimetry (photo-DSC) assessed the overall polymerization rates in an inert nitrogen atmosphere at 25°C. The photo-DSC used was a Mettler-Toledo DSC822^e modified with a Hamamatsu Lightning Cure 200 UV-spot light source (a high pressure mercury arc lamp). The samples (2 μL) were purged with nitrogen for 3 min and thereafter irradiated ($I_o = 50$ mW/cm^2) for an additional 4 min until the polymerization was complete.

RESULTS AND DISCUSSION

Syntheses

The half-adduct structures were characterized by ^{1}H-NMR and ^{13}C-NMR spectroscopy; however, IR spectroscopy provides structural differentiation of the half-adducts and the CoBOC

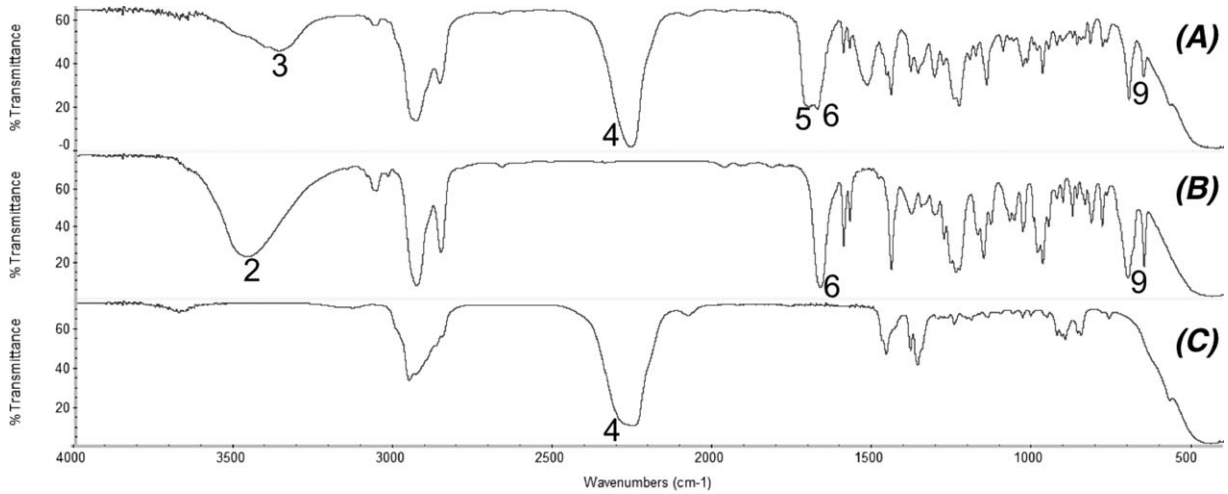

Figure 3. FT-IR spectral comparison of (A) HCPK-IPDI half-adduct with (B) HCPK and (C) IPDI.

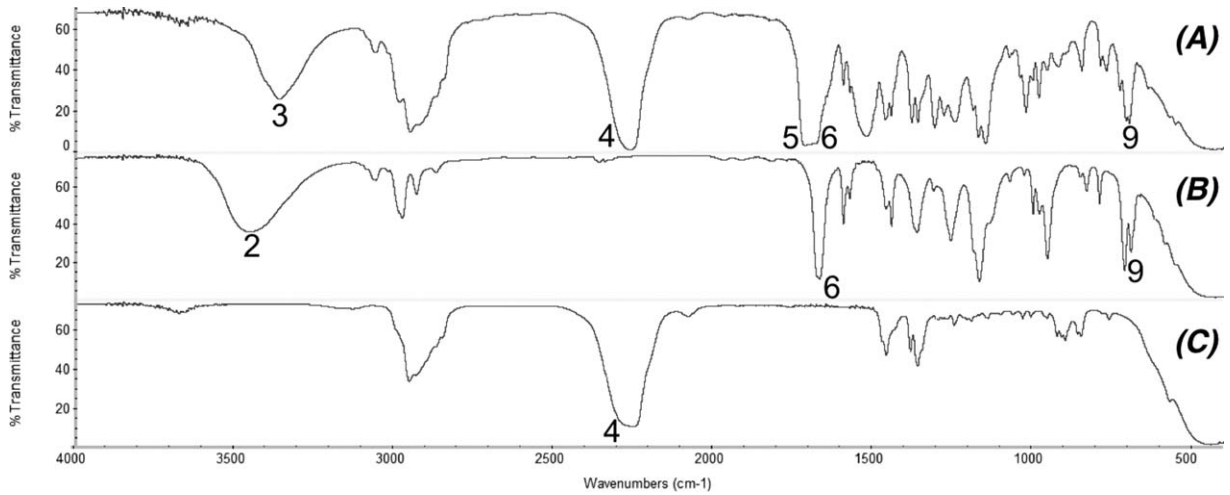

Figure 4. FT-IR spectral comparison of (A) HDMAP-IPDI half-adduct with (B) HDMAP and (C) IPDI.

photoinitiators. Table II provides relevant IR peak locations for differentiating synthetic products.

Figure 3 differentiates the HCPK-IPDI half-adduct from both HCPK and IPDI; Figure 4 similarly characterizes the HDMAP-IPDI half-adduct. Peak 2 shows the hydrogen bonded hydroxyl stretch of the alcohol from the photoinitiator (HCPK in Figure 3 and HDMAP in Figure 4) with Peak 4 confirming the presence of the isocyanate groups on both the half-adduct and IPDI. The carbonyl of the photoinitiators are demarcated by Peak 6. The hydrogen bonded hydroxyl stretch (Peak 2) of both photoinitiators do not persist in the half-adducts while the isocyanate Peak 4 is noticeably diminished (i.e., is not as broad) indicating that a significant portion (i.e., approximately 50% based on stoichiometry) of the isocyanate groups have reacted with the alcohol of the photoinitiators. Furthermore, Peaks 3 and 5 provide evidence for the formation of the urethane linkage.

The CoBOC photoinitiator was characterized via solid-state IR (1% material in KBr; pelletized) and compared to both the half-adduct and the unmodified clay. Comparing the IR of the HCPK-IPDI-C93A CoBOC photoinitiator to that of the HCPK-IPDI half-adduct and C93A, the disappearance of the isocyanate Peak 4 and the significant reduction of the structural hydroxyl stretch at approximately 3628 cm^{-1} (Peak 1) indicate that the half-adduct has reacted with the structural hydroxyls (i.e., the OH groups on the exterior of the clay platelets) to form a urethane linkage (Figure 5).

The HDMAP-IPDI-C93A CoBOC photoinitiator IR comparison (Figure 6) resembles that of the HCPK-IPDI-C93A CoBOC photoinitiator; however, the isocyanate (Peak 4) of the half-adduct did not completely react with the clay perhaps due to stoichiometric causation evidenced by the diminished structural hydroxyl Peak 1 of the clay.

ED-XRF was used to determine the percent by weight of the organic composition of the CoBOC photoinitiator, HCPK-IPDI-C93A, relative to the C93A composition. For C93A, the weight percent composition of Al, Si, and C, H, N, O was determined to be 10.9, 32.3, and 50.59, respectively; the weight

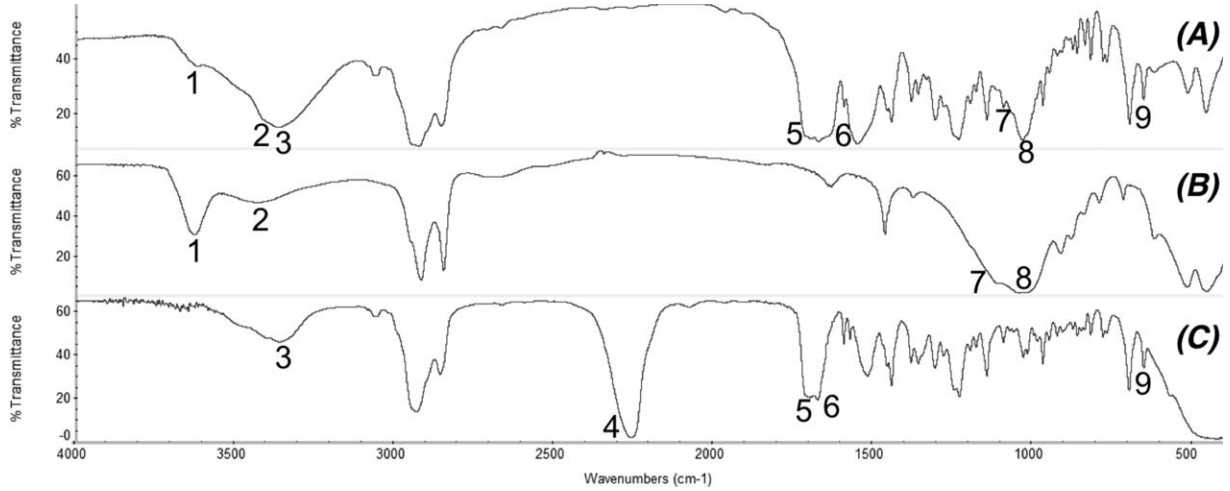

Figure 5. FT-IR spectral comparison of (A) HCPK-IPDI-C93A CoBOC photoinitiator with (B) C93A and (C) HCPK-IPDI half-adduct.

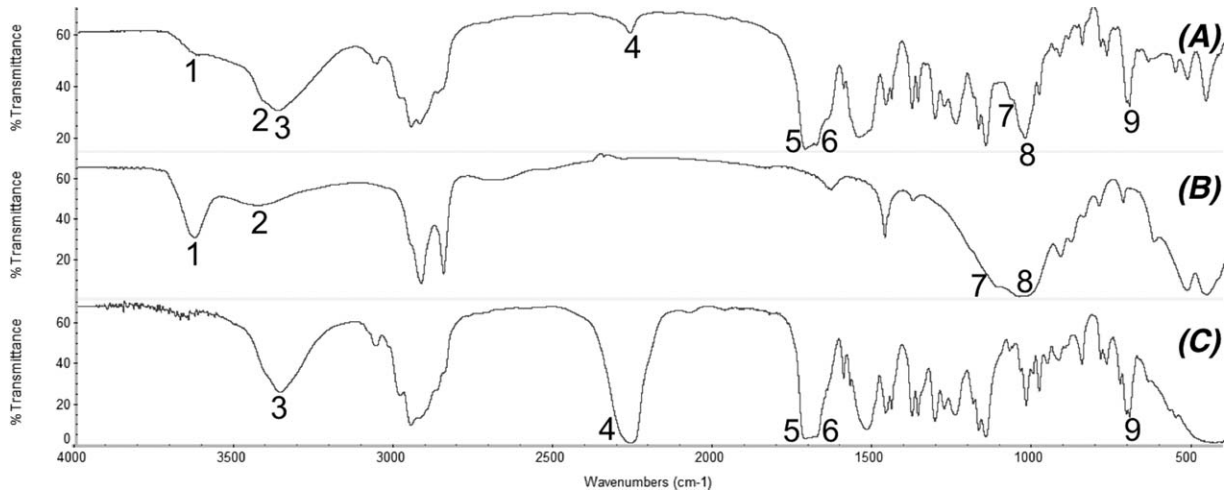

Figure 6. FT-IR spectral comparison of (A) HDMAP-IPDI-C93A CoBOC photoinitiator with (B) C93A and (C) HDMAP-IPDI half-adduct.

percent composition of Al, Si, and C, H, N, O for HCPK-IPDI-C93A was determined to be 8.46, 29.17, and 57.62, respectively. The ratio of C, H, N, O relative to the sum of Al and Si in the sample were determined using the following equations:

$$x = \frac{\%_{\text{organic}}^{\text{C93A}}}{\%_{\text{Al}}^{\text{C93A}} + \%_{\text{Si}}^{\text{C93A}}} \quad (1)$$

$$y = \frac{\%_{\text{organic}}^{\text{HCPK-IPDI-C93A}}}{\%_{\text{Al}}^{\text{HCPK-IPDI-C93A}} + \%_{\text{Si}}^{\text{HCPK-IPDI-C93A}}} \quad (2)$$

To factor out the contribution of C93A in HCPK-IPDI-C93A, Equation (3) was used whereupon the increase in organic composition was found to be 31.3% by weight.

$$\%_{\text{organic}}^{\text{increase}} = \left(\frac{y-x}{x}\right) \times 100\% \quad (3)$$

Therefore, HCPK-IPDI was incorporated onto C93A at a ratio of 7.35×10^{-4} mole/g of HCPK-IPDI-C93A.

Physical Characterization

The goal of any coating additive (e.g., a clay composite material) is to improve one of more properties; therefore, several coatings were physically characterized for adhesion, hardness, impact flexibility, and flexibility. Also, cure time was qualitatively evaluated for each of the coatings when line cured as described previously. HCPK initiated formulations were examined for the aforementioned properties and tabulated in Table III.

Crosshatch adhesion did not vary for any of the samples indicating that the formulation did not exhibit a high degree of adhesion to the metal substrate. Pencil hardness progressively improved on incorporation of both the clay additive and the CoBOC photoinitiator with the latter providing the best hardness. Impact flexibility, both direct and reverse, was decreased with the addition of clay and CoBOC photoinitiator (equivalent weight percentages) perhaps due to the physical disruption and adhesion deficiency of the coating due to the clay and CoBOC photoinitiator. Compressive flexibility decreased with the addition of clay and CoBOC photoinitiator, though the compressive flexibility of the coating comprised, in part, of the CoBOC photoinitiator was nominally improved relative to the coating incorporating the clay additive. Flexibility based on elongation of the coating remained consistent for the sample set with elimination of microcracking of the coating incorporating the CoBOC photoinitiator. Therefore, adhesion was negatively affected by the addition of the clay and CoBOC photoinitiator while hardness was enhanced, as expected. Furthermore, the clay additive formulation required more passes through the cure line due to the clay acting as a physical impediment to polymerization while the formulation containing the CoBOC photoinitiator required only one extra pass to obtain complete cure, indicating that, though the CoBOC photoinitiator is a physical polymerization impediment, the centering of the initiating events on the clay seem to balance out the impediment effect.

Likewise, select physical properties (e.g., adhesion, hardness, impact flexibility, and flexibility) were evaluated for the HDMAP initiated formulations (Table III). Qualitative comparisons of cure time were also examined and tabulated in Table IV.

Table III. Physical Characterization of HCPK Initiated Formulations (2 : 1 AUDA to TMPTA): α, 1% HCPK; γ, 1% HCPK and 2% C93A; and ε 2% HCPK-IPDI-C93A

Physical characterization	ASTM	α	γ	ε
Crosshatch adhesion	D 3359-08	0B	0B	0B
Pencil hardness	D 3363-05	4B	HB	6H
Impact flexibility, direct[a]	D 6905-03	16[d]	6[d]	4[d]
Impact flexibility, reverse[a]	D 6905-03	16[d]	2[cd]	2[cd]
Flexibility, compression[b]	D 522-93a	31[d]	20[d]	21[d]
Flexibility, elongation[b]	D 522-93a	32[de]	32[de]	32[d]
Passes (21 ft/min)	N/A	9	14	10

[a] Units in/lbs.
[b] In percent.
[c] Through-cracked.
[d] Delaminated.
[e] Microcracked.

Table IV. Physical Characterization of HDMAP Initiated Formulations (2 : 1 AUDA to TMPTA): β, 1% HDMAP; δ, 1% HDMAP and 2% C93A; and ζ, 2% HDMAP-IPDI-C93A

Physical Characterization	ASTM	β	δ	ζ
Crosshatch adhesion	D 3359-08	0B	0B	0B
Pencil hardness	D 3363-05	2B	2B	4H
Impact flexibility, direct[a]	D 6905-03	18[d]	18[d]	20[d]
Impact flexibility, reverse[a]	D 6905-03	12[d]	2[cd]	6[d]
Flexibility, compression[b]	D 522-93a	9[d]	11[d]	32[d]
Flexibility, elongation[b]	D 522-93a	32[de]	32[d]	32[de]
Passes (21 ft/min)	N/A	9	12	10

[a] Units in/lbs.
[b] In percent.
[c] Through-cracked.
[d] Delaminated.
[e] Microcracked.

Generally, the HDMAP initiated formulations showed improved physical properties with the exception of crosshatch adhesion which remained unchanged. Pencil hardness and impact flexibility (direct) were improved for the HDMAP-based CoBOC photoinitiator relative to both the HDMAP and HDMAP/clay samples. Reverse impact flexibility decreased for both clay and CoBOC photoinitiator samples relative to the HDMAP only sample, though the CoBOC photoinitiator sample was improved compared to the clay additive. The compressive flexibility was enhanced for both the clay additive and the CoBOC photoinitiator with respect to the HDMAP only sample while the flexibility of an elongated sample remained consistently high for all samples. The qualitative cure time was decreased for the samples containing the clay additive and CoBOC photoinitiator; however, the CoBOC photoinitiator had a marked improvement in qualitative cure time relative to the clay additive sample.

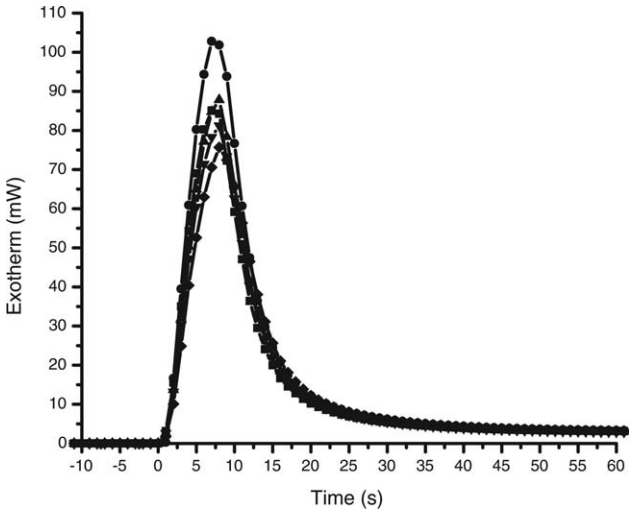

Figure 7. Photo-DSC of 0.5 wt % HCPK in HDODA with varying C93A concentration (2 μL sample, $I_o = 50$ mW/cm^2, 3-min N_2 purge, full arc): 0.5% HCPK in HDODA (■); 0.5% C93A, 0.5% HCPK in HDODA (•); 1% C93A, 0.5% HCPK in HDODA (▲); 2% C93A, 0.5% HCPK in HDODA (▼); and 5% C93A, 0.5% HCPK in HDODA (◆).

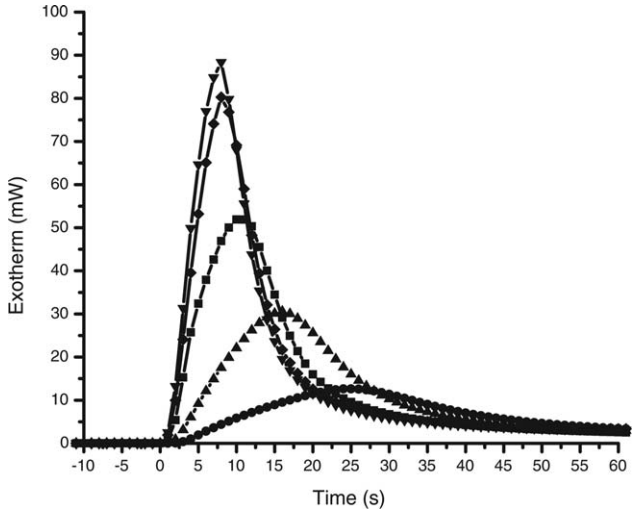

Figure 8. Photo-DSC of varying HCPK-IPDI-C93A concentration and compared to 0.155 wt % HCPK in HDODA (2 μL sample, $I_o = 50$ mW/cm^2, 3-min N_2 purge, full arc): 0.155% HCPK in HDODA (■); 0.5% HCPK-IPDI-C93A in HDODA (•); 1% HCPK-IPDI-C93A in HDODA (▲); 2% HCPK-IPDI-C93A in HDODA (▼); and 5% HCPK-IPDI-C93A in HDODA (◆).

Kinetic Characterization

Initially, photo-DSC was employed for a comparative polymerization rate study with a static photoinitiator concentration and varying C93A concentration in 1,6-hexanediol diacrylate (HDODA). The variable C93A addition (i.e., 0.5, 1, 2, and 5 wt %) in the controls indicated that the clay scattered and/or absorbed the incident UV radiation thereby producing a progressively decreasing polymerization rate as C93A concentration increased.[35] The HDMAP/C93A control experiment exhibited results similar to that of HCPK/C93A shown in Figure 7.

After demonstrating the anticipated inverse relationship between clay concentration and photopolymerization rate, the HCPK-based CoBOC photoinitiator was kinetically characterized to determine the polymerization rate (Figure 8). The control sample (i.e., 0.155 wt % HCPK) was calculated based on the molar percent incorporation of HCPK assuming similar organomodification reported by Lv *et al.*[2] Full arc irradiation demonstrated that increasing concentration of the HCPK-based CoBOC photoinitiator yielded increasing photopolymerization rates.

The exception to the trend is the 5% by weight HCPK-based CoBOC where the polymerization rate seemed to decrease, perhaps due to a compatibility issue with the polymerizable media (HDODA) typical of greater concentrations of clay-based additives which can scatter/absorb incident light. The HCPK-based CoBOC acted as an effective photoinitiator and demonstrated the unique, direct relationship between clay concentration and photopolymerization rate.

The synthesized HDMAP-based CoBOC photoinitiator was also examined via photo-DSC and demonstrated that increased concentrations of the HDMAP-based CoBOC photoinitiator yielded an increased polymerization rate (Figure 9).

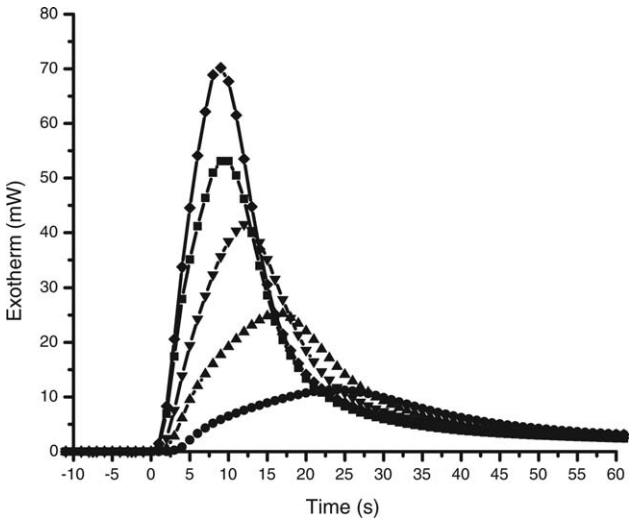

Figure 9. Photo-DSC of varying HDMAP-IPDI-C93A concentration and compared to 0.238 wt % HDMAP in HDODA (2 μL sample, $I_o = 50$ mW/cm^2, 3-min N_2 purge, full arc): 0.238% HDMAP in HDODA (■); 0.5% HDMAP-IPDI-C93A in HDODA (•); 1% HDMAP-IPDI-C93A in HDODA (▲); 2% HDMAP-IPDI-C93A in HDODA (▼); and 5% HDMAP-IPDI-C93A in HDODA (◆).

Comparing the CoBOC photoinitiators with the controls, the controls showed that increased clay concentrations reduced the polymerization rate, likely due to scattering/absorption of incident light by the clay. However, the CoBOC photoinitiators generally yield an increasing trend for the polymerization rate relative to the controls (0.5% photoinitiator and 0.5–5% C93A in HDODA), a behavior likely attributable to immobilization of propagating radicals thereby reducing termination by radical combination and resembling autoacceleration in crosslinked polymer matrices.[8] With increasing concentrations of the CoBOC photoinitiator the overall polymerization rate is enhanced thereby overcoming the scattering/absorptive effect of the clay filler. Furthermore, formulating clay composite materials may be simplified for UV-curable materials by combining the photoinitiator and clay composite into a single formulation component.

CONCLUSIONS

Barrier coatings are the limiting technology for many organic components in electronics and thus highly researched. Therefore, we have designed and characterized a series of novel, covalently bound organomodified clay (CoBOC) photoinitiators where the photoinitiating component is covalently bound to the clay via the hydroxyl-isocyanate reaction to form a urethane. Structures of the half-adducts (i.e., photoinitiator-IPDI) were confirmed via IR, ^{1}H-NMR, and ^{13}C-NMR while the full adduct (i.e., photoinitiator-IPDI-clay) was analyzed via solid-state IR to show the disappearance of the clay's structural hydroxyls and the half-adduct's remaining isocyanate groups. Physical characterization (e.g., adhesion, hardness, impact flexibility, and flexibility) gave diverse results with increased hardness for both CoBOC photoinitiators. The HCPK CoBOC photoinitiator had diminished impact flexibility and compressive flexibility relative to the control; the HDMAP CoBOC photoinitiator had decreased reverse impact flexibility but improved direct impact flexibility and compressive flexibility. The polymerization rate, as determined via photo-DSC, was decreased with increasing clay concentrations when initiated with both HCPK and HDMAP; however, the polymerization rate was enhanced with increasing concentrations of either CoBOC photoinitiator. Therefore, the CoBOC photoinitiators were determined to be effective composite photoinitiators with the potential to act as physical impediments to water and/or oxygen permeation in barrier coatings for electronic applications.

ACKNOWLEDGMENTS

The authors would like to acknowledge funding from both the Welch Foundation (Grant #: R-0021) and Abilene Christian University's Office of Research and Sponsored Programs and would also like to thank IGM Resins, Southern Clay Products, and Bayer Material Science for material provision.

REFERENCES

1. Zervos, H. Barrier Films for Flexible Electronics: Needs, Players & Opportunities. IDTechEx, Ltd, **2009**.
2. Lv, S.; Zhou, W.; Li, S.; Shi, W. *Eur. Polym. J.* **2008**, *44*, 1613.
3. Jlassi, K.; Singh, A.; Aswal, D. K.; Losno, R.; Benna-Zayani, M.; Chehimi, M. M. *Colloids Surf. Physicochem. Eng. Asp.* **2013**, *439*, 193.
4. Owusu-Adom, K.; Guymon, C. A. *Macromolecules* **2009**, *42*, 180.
5. Kim, S. K.; Baguenard, C.; Guymon, C. A. *Macromol. Symp.* **2013**, *329*, 173.
6. Tan, H.; Nie, J. *Macromol. React. Eng.* **2007**, *1*, 384.
7. Tan, H.; Ma, G.; Xiao, M.; Nie, J. *Polym. Compos.* **2009**, *30*, 612.
8. Kim, S. K.; Guymon, C. A. *J. Polym. Sci. Part A Polym. Chem.* **2011**, *49*, 465.
9. Tan, H.; Yang, D.; Han, J.; Xiao, M.; Nie, J. *Appl. Clay Sci.* **2008**, *42*, 25.
10. Rigoli, I. C.; Batista, T.; Cavalheiro, C. C. S.; Neumann, M. G. *Macromol. Symp.* **2010**, *298*, 138.
11. Keller, L.; Decker, C.; Zahouily, K.; Benfarhi, S.; Le Meins, J. M.; Miehe-Brendle, J. *Polymer* **2004**, *45*, 7437.
12. Shemper, B. S.; Morizur, J.-F.; Alirol, M.; Domenech, A.; Hulin, V.; Mathias, L. J. *J. Appl. Polym. Sci.* **2004**, *93*, 1252.
13. Peila, R.; Malucelli, G.; Lazzari, M.; Priola, A. *Polym. Eng. Sci.* **2010**, *50*, 1400.
14. Bae, J. *Polym. Int.* **2012**, *61*, 895.
15. Jiratumnukul, N.; Intarat, R. *J. Appl. Polym. Sci.* **2008**, *110*, 2164.
16. Nese, A.; Sen, S.; Tasdelen, M. A.; Nugay, N.; Yagci, Y. *Macromol. Chem. Phys.* **2006**, *207*, 820.
17. Tan, H.; Nie, J. *J. Appl. Polym. Sci.* **2007**, *106*, 2656.

18. Qin, X.; Wu, Y.; Wang, K.; Tan, H.; Nie, J. *Appl. Clay Sci.* **2009**, *45*, 133.
19. Salmi, Z.; Benzarti, K.; Chehimi, M. M. *Langmuir* **2013**, *29*, 13323.
20. Altinkok, C.; Uyar, T.; Tasdelen, M. A.; Yagci, Y. *J. Polym. Sci. Part Polym. Chem.* **2011**, *49*, 3658.
21. Oral, A.; Tasdelen, M. A.; Demirel, A. L.; Yagci, Y. *J. Polym. Sci. Part Polym. Chem.* **2009**, *47*, 5328.
22. Lee, S.-S.; Kim, J. *J. Polym. Sci. Part B Polym. Phys.* **2004**, *42*, 2367.
23. Inceoglu, F.; Dalgicdir, C.; Menceloglu, Y. Z. Nanotechnology Applications in Coatings; ACS Symposium Series; American Chemical Society: Washington, **2009**; Vol. 1008, p 255.
24. Pavlacky, E.; Ravindran, N.; Webster, D. C. *J. Appl. Polym. Sci.* **2012**, *125*, 3836.
25. Valandro, S. R.; Poli, A. L.; Neumann, M. G.; Schmitt, C. C. *Appl. Clay Sci.* **2013**, *85*, 19.
26. Kim, Y. H.; Kim, D. S. *Polym. Adv. Technol.* **2008**, *19*, 1236.
27. Uhl, F. M.; Davuluri, S. P.; Wong, S.-C.; Webster, D. C. *Chem. Mater.* **2004**, *16*, 1135.
28. Pavlacky, E.; Webster, D. C. *J. Appl. Polym. Sci.* **2013**, *129*, 324.
29. Kim, Y. H.; Kim, D. S. *Polym. Compos.* **2009**, *30*, 926.
30. Asif, A.; Huang, C.; Shi, W. *Colloid Polym. Sci.* **2004**, *283*, 200.
31. ASTM D3363-05 Standard Test Method for Film Hardness by Pencil Test, **2011**.
32. ASTM D6905-03 Standard Test Method for Impact Flexibility of Organic Coatings, **2012**.
33. ASTM D3359-08 Standard Test Methods for Measuring Adhesion by Tape Test, **2008**.
34. ASTM D522-93a Standard Test Methods for Mandrel Bend Test of Attached Organic Coatings, **2008**.
35. Davidenko, N.; García, O.; Sastre, R. *J. Appl. Polym. Sci.* **2005**, *97*, 1016.